Original Research Article

Online adaptive dose restoration in intensity modulated proton therapy of lung cancer to account for inter-fractional density changes

Elena Borderías Villarroel[a,*], Xavier Geets[a,b], Edmond Sterpin[a,c]

[a] UCLouvain, Molecular Imaging-Radiotherapy and Oncology (MIRO), Brussels, Belgium
[b] Cliniques Universitaires Saint-Luc, Department of Radiation Oncology, Brussels, Belgium
[c] KU Leuven, Department of Oncology, Laboratory of Experimental Radiotherapy, Leuven, Belgium

ABSTRACT

Background and purpose: In proton therapy, inter-fractional density changes can severely compromise the effective delivery of the planned dose. Such dose distortion effects can be accounted for by treatment plan adaptation, that requires considerable automation for widespread implementation in clinics. In this study, the clinical benefit of an automatic online adaptive strategy called dose restoration (DR) was investigated. Our objective was to assess to what extent DR could replace the need for a comprehensive offline adaptive strategy.

Materials and methods: The fully automatic and robust DR workflow was evaluated in a cohort of 14 lung IMPT patients that had a planning-CT and two repeated 4D-CTs (rCT1,rCT2). Initial plans were generated using 4D-robust optimization (including breathing-motion, setup and range errors). DR relied on isodose contours generated from the initial dose and associated patient specific weighted objectives to mimic this initial dose in repeated-CTs. These isodose contours, with their corresponding objectives, were used during re-optimization to compensate proton range distortions disregarding re-contouring. Robustness evaluations were performed for the initial, not-adapted and restored (adapted) plans.

Results: The resulting DVH-bands showed overall improvement in DVH metrics and robustness levels for restored plans, with respect to not-adapted plans. According to CTV coverage criteria (D95% > 95%Dprescription) in not-adapted plans, 35% (5/14) of the cases needed offline adaptation. After DR, Median(D95%) was increased by 1.1 [IQR,0.4] Gy and only one patient out of 14 (7%) still needed offline adaptation because of important anatomical changes.

Conclusions: DR has the potential to improve CTV coverage and reduce offline adaptation rate.

1. Introduction

The sharp distal dose fall-off of the proton beams makes proton therapy (PT) an attractive alternative to conventional X-ray radiotherapy (XT). In particular, lung cancer patients may benefit from PT, as critical organs at risk (OAR) like the heart and oesophagus may surround the target. Studies showed that, compared to XT, intensity-modulated proton therapy (IMPT) has potential to improve OAR sparing whilst maintaining, or even increasing the prescribed dose to the target. [1–5] and thus lead to better clinical outcomes i.e. less toxicity and higher survival rates [6–10].

The sharp dose gradients produced by IMPT yields dose distributions with increased sensitivity to treatment uncertainties such as patient setup, inter- and intra-fractional anatomical variations [11,12]. This issue should not be addressed as typically done in XT, i.e.

expansion of the clinical target volume (CTV) with safety margins leading to the planning target volume (PTV). The main reason is the invalidity in PT of the static dose cloud approximation underlying the PTV margin recipes. Therefore, more complex treatment planning procedures have been introduced such as robust optimization (RO) [13–17], where uncertainties are simulated during plan optimization. The interplay between respiratory and scanning motions must also be addressed cautiously, for instance using rescanning [18,19].

Unfortunately, RO has several limitations. It is a computationally-intensive procedure, based on uncertainty parameters that are not patient specific (setup and range errors), which typically excludes important types of errors like day-to-day anatomical variations. However, those anatomical variations may have a critical impact, since about 30% of IMPT lung patients require adaptive planning even though they were initially planned using RO [5,20]. Furthermore, some studies

---

* Corresponding author at: Université catholique de Louvain (UCLouvain), Molecular Imaging, Radiotherapy and Oncology (MIRO), Avenue Hippocrate 54, Bte B1.54.07, 1200 Brussels, Belgium.
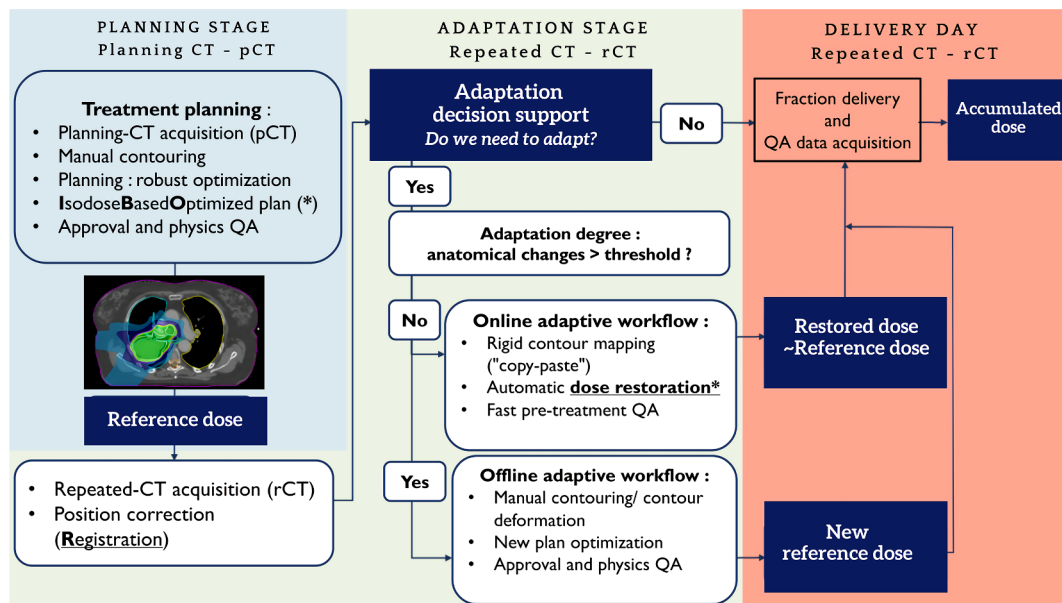*E-mail address:* elena.borderias@uclouvain.be (E. Borderías Villarroel).

Fig. 1. Example of the proposed adaptive workflow, which combines offline and online-adaptive strategies including dose restoration to perform optimal IMPT proton treatment. Three different stages are presented in this workflow: planning, adaptation and delivery day. If online adaptation strategy is chosen, the adaptation stage is performed on the delivery day. (*): IBO-plan is the key that automatizes dose restoration re-optimization.

report that adaptation is highly recommended [17] or even mandatory [21] for advanced lung cancer treated with IMPT, since it ensures target coverage and improves treatment accuracy from a dosimetric point-of-view.

The degradation of plan quality observed in PT is caused by 1) dose distortions due to density changes along the beam path (PT specific) and 2) relative movement between anatomical structures. In order to handle both issues, a full adaptative workflow is necessary. However, its implementation requires considerable automation for a practical usage in clinical practice, typically characterized by tight clinical workflows. Automation is not straightforward, as it requires the generation of reliable new contours and a new plan, together with their associated verification and approval. The lack of automation is one of the key reasons preventing the deployment of online adaptive on a wide scale [22,23].

As an alternative, dose distortions caused by density changes could be compensated by restoring the clinically approved planned dose. This approach, called 'dose restoration' (DR), was first introduced for online adaptation of prostate cancer [24], and later tested for head-and-neck and one lung tumors [25]. DR aims at reproducing the planned dose using density information from the new (repeated) CT, by generating a new (restored) plan with updated proton beam energies and spot weights, thereby removing the need for contour deformations. In such approach, automation was facilitated. Differences in dose distributions can indeed be quantified without qualitative evaluation by an expert, which is not the case for auto-segmentation. However, the clinical value and robustness of DR in lung remains to be assessed on a larger patient cohort. In this study, we evaluated the clinical value of the restoration workflow for 14 lung IMPT patients. Limitations with respect to a full adaptive workflow, where changes in relative positions and shapes of anatomical structures are considered, were also addressed.

2. Methods and materials

2.1. Patients

Fourteen lung cancer patients treated with photons were re-planned retrospectively using IMPT. A 4D-planning-CT and two repeated 4D-CTs (rCT1, rCT2) acquired systematically after 2 and 4 weeks of

radiotherapy were available for each patient. For patient 9, rCT2 was missing. Patients were representative of a patient population with different tumor sizes (79–433 cm^3) and motion amplitudes (1.1–11.1 mm), more characteristics can be found in the supplementary material Table S1. A joint ethical committee of Cliniques Universitaires St. Luc and UCLouvain approved the collection of the retrospective data used in this study.

2.2. Treatment planning strategy

Following the European Oganization for Research and Treatment of Cancer (EORTC) protocol [26], a 5 mm expansion was applied to the GTV (Gross Tumor Volume) to create the CTV, and corrected to account for anatomical boundaries. The treatment planning system (TPS) RayStation 8A (RaySearch) was used to perform 4D worst-case robust optimization against breathing motion, setup and range errors. Robust parameters of 5 mm and 3% for setup and range errors, respectively, were used and extracted from literature [13,27,28]. Motion was modelled by using 3 images: the mid-position-CT (MidP-CT), used as planning CT, together with the end-inhale and end-exhale breathing phases [29]. This combination of motion, setup and range errors led to 63 optimization scenarios : 7 (setup: ± 5mm in x,y,z directions plus nominal scenario) × 3 (density: ± 3%,0%) × 3 (three breathing-phases).The treatment plans were optimized using pencil beam dose engine (v4.2) and setting robust maximum and minimum objectives on the CTV. TPS calculations/optimizations were run on 2 Intel(R) Xeon(R) CPU-E5-2643-v3 3.40 GHz processors with 64 GB of RAM. A relative biological effectiveness (RBE) of 1.1 was assumed. The prescribed dose (Dp) to the CTV was 66 Gy (33x2 Gy).

2.3. Simplified adaptive workflow

Fig. 1 illustrates the proposed adaptive workflow, including the online adaptive branch with automatic dose restoration that did not require re-contouring on rCTs. The dose restoration approach used here was the "isodose volume dose restoration", introduced by Bernatowicz et al.[25]. For preparing the dose restoration, an additional step was performed during the planning stage compared to a regular planning procedure (see Section 2.4). Online dose restoration must be automatic,

fast (patient is lying on the couch) and accurate (generates high quality plans that minimize the physician approval step). It is important to remember that dose restoration only addressed distortions due to density changes. DR can account for tumor shrinkage for example, while for large tissue deformations and geometrical reorganization of the anatomy, an offline adaptation is necessary.

2.4. Planning stage: Isodose based optimized plan

First, a set of isodose volumes was constructed from the initial dose distribution obtained using the method described in section 2.2. Isodose volumes were created every 2 Gy within 95%–107% of the prescription dose and 5 Gy outside. Subsequently, an isodose-based optimization (IBO) was performed using a pair of minimum and maximum objectives for each isodose volume. Finally, the objective weights were manually adjusted in order to match IBO and initial plan DVHs. The objectives at isodoses corresponding to dose prescription were set as robust, using the initial robustness parameters (5 mm/3%/3phases). The resulting weighted objectives were saved in a patient-specific template, which served later to optimize the restored plan. Hence, each patient had two plans at the planning stage: the initial and the IBO plan. We assumed the IBO dose as the approved and delivered reference dose since the IBO and initial dose distributions were equivalent i.e. they both met clinical goals and presented overlapping DVHs.

2.5. Treatment day: Registration, ROI mapping and re-optimization

Bony-anatomy based rigid registration was performed between planning MidP-CTs and repeated MidP-CTs for patient positioning. Bony matching has been historically used in PT clinical routine to reproduce the relative position of bones with respect to protons [30,31]. Using the registration matrix, contours (isodoses, OARs and target) were mapped from the planning MidP-CT to the repeated MidP-CTs. Afterwards, the previously calculated IBO template was used to re-optimize the plan.

2.6. Evaluation metrics

The impact of density changes was analysed by evaluating the treatment plans on two repeated 4D-CTs (rCT1, rCT2). The reference plans (IBO-plans), were recalculated on repeated-CTs. Not adapted dose distributions were compared to restored doses using dose-volume parameters such as D95%(CTV) (dose received by 95% of the target volume), and the homogeneity index HI ($=$(D95%-D5%)/D50%). Clinical limit for target coverage was defined at 95% of the prescribed dose, i.e. D95%(CTV) $>$ 95%Dp (66 Gy) $=$ 62.7 Gy.

For robustness evaluation, the reference (IBO), restored and not adapted plans were re-computed in the same 63 scenarios used for optimization (5 mm/3%/3phases) using RayStation dose perturbation tool. The DVHs from the 63 simulated uncertainty scenarios were grouped into DVH-bands. The bandwidth served to measure the robustness level. Propagation of the robustness level through dose restoration was analysed. For each DVH-metric (D95%(CTV), D2%(SpinalCord) or mean dose in OARs) nominal and worst-case scenarios values were reported. Differences respect to the reference dose were compared for not adapted and restored plans.

Dose-volume parameters and robustness were evaluated in the rigidly mapped contours (RS_map) and in the contours (OARs and targets) recontoured by an experienced radiation oncologist. This last set will from this point onward be denoted as 'real' structures (RS_real). Evaluations were performed for the two repeated-CTs (rCT1,rCT2).

DICE similarity coefficient was calculated between CTV_map and CTV_real to quantify the accuracy of the rigid registration between planning and repeated-CTs (Supplementary material Table.S2). This statistical tool which measures the similarity between two data sets X,Y $(2|X\cap Y|/(|X|+|Y|))$ is often used to evaluate the accuracy of

segmentation methods.

To ensure a reliable and accurate dose mimicking, we also analysed local differences respect to the reference (IBO) dose in four different dose level regions (prescribed, high, medium and low dose) following Bernatowicz et al.(2018)[25]. Subtractions between the evaluated (not adapted/adapted) and reference doses were performed. Absolute dose difference at 2% of the volume was reported for each region (for instance DE(vol $=$ 2%) $=$ 5 Gy means that only 2% of the volume may have a dose difference superior to 5 Gy). This metric characterized the near maximum absolute dose error.

Analysis were performed using boxplots calculated with values of the 14 patients. Medians [interquartile range(IQR)] from not adapted versus restored doses in rCT1 and rCT2 were reported and compared using Wilcoxon signed-rank test (paired difference test), in order to assess the statistical significance. Differences between not adapted and restored metrics where considered statistically significant for a p-value $<$ 0.05.

3. Results

3.1. Target coverage and homogeneity index

Fig. 2 presents D95%(CTV) and homogeneity index (HI) values evaluated in the nominal scenario, which represents the scenario without added uncertainty. Even in this case, 35% (5/14) in rCT1 and 23% (3/13) in rCT2 of patients would have benefit from adaptation to ensure clinical acceptable target coverage.

As observed in Fig. 2, reference plans were significantly distorted without adaptation, leading to CTV underdosage and higher HI in both repeated-CTs. Both metrics were improved after restoration, showing that DR can deal with over/under-dosages.

Without adaptation, in RS_map, Median(D95%(CTV)) was reduced from 65.2[0.5] Gy to 63.7[1.39] Gy (rCT1) and to 64.2[1.28] Gy (rCT2). For the RS_real, Median(D95%(CTV)) fell to 63.6[3.4] Gy (rCT1) and 63.6 [1.4] Gy (rCT2). After restoration, target coverage was also re-established increasing Median(D95%(CTV)) to 65.1[0.4] Gy (rCT1) and to 65.0[0.5] Gy (rCT2) in RS_map and to 64.5 [2.0] Gy (rCT1) and to 64.7[1.3] Gy in RS_real. In all restored cases (RS_map and RS_real), D95%(CTV) values were maintained within clinical limits, except for RS_real in patient 6. In this case, the rigid registration failed due to substantial differences in the anatomy. As a result, the RS_real did not match RS_map (DICE coefficient 0.36 (rCT1) and 0.32 (rCT2)), and the initial dose was reproduced in the wrong location. Only in this case, offline adaptation was absolutely needed to ensure CTV coverage.

3.2. Robustness evaluation

Fig. 3 shows the deviations from the reference dose for not adapted and restored plans in nominal and wort-case scenarios for D95% (CTV), D2% (SpinalCord) and MeanDose (Lung/Heart/Esophagus). After adaptation, median values were closer to zero, indicating that the reproduction of the initial dose was improved. Some OARs (e.g. spinal cord) even got lower doses. Adapted plans also showed improved results in worst-case DVH-metrics.

Larger variabilities were observed in RS_real (Fig. 3.c and d) compared to RS_map (Fig. 3.a and b). However, in both contour sets, all restorations improved target coverage and recovered OARs metrics to original values. The number of outliers increased in RS_real, with most outliers corresponding to patient 6, who had significant CTV underdosage and heart overdosage.

Outliers representing an overdosage in the esophagus on rCT2 (Fig. 3.d) were associated to the entrance of the esophagus into a high dose region, caused by tumor shrinkage. Underdosage in the CTV and overdosage in D2(PRV SC)-worst-case in rCT2 (Fig. 3.d) correspond to patient 8. In this case, the robustness level was not achieved in rCT2, being translated into a wider CTV DVH-band. This is probably due to
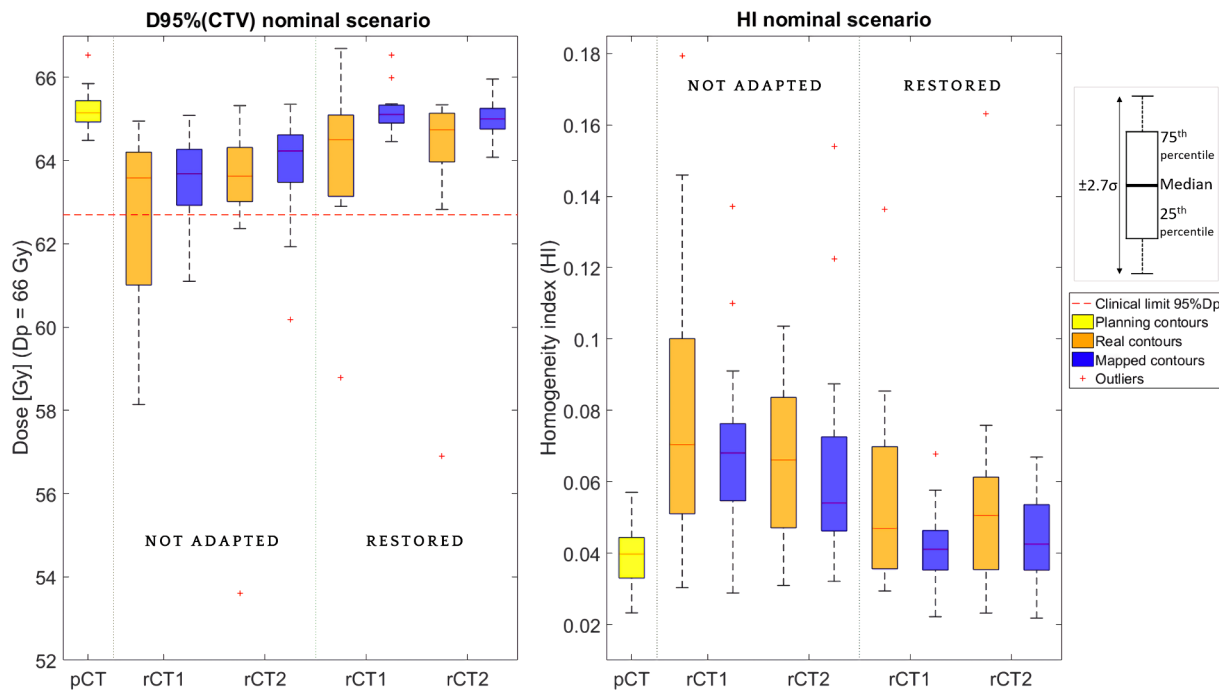
Fig. 2. D95%(CTV) (dose received at 95% of the CTV volume) and homogeneity index values from nominal scenario are represented using boxplots. The nominal scenario stand for doses without any simulated uncertainty, which means without robust assessment. Each boxplot contains the 14 patient's information for a certain plan (not adapted/restored) evaluated on different images: planning CT and two repeated-CTs. Blue and orange boxes correspond to RS_map contours (rigidly mapped) and RS_real contours respectively. The clinical limit is achieved if dose received at D95%(CTV) is higher than 95%(Dp(66 Gy)) = 62.7 Gy . *Abbreviations: Dp = Prescribed dose, HI = Homogeneity index, pCT = planning CT , rCT1 = first repeated CT , rCT2 = second repeated CT.* (For interpretation of the references to colour in this figure legend, the reader is referred to the web version of this article.)

contour miss-alignment characterized with a DICE coefficient of 0.67.

There was no significant dose difference for lung, heart and eso-phagus between not adapted and restored plans (p > 0.05) However statistical significance (p < 0.05) was observed in target coverage and maximum dose (D2%) in the spinal cord, for nominal and worst-case values (see Table.1).

Fig. 4 shows an example (Patient 9) of CTV underdosage close to clinical limit, causing the robustness test to fail. After DR, target cov-erage was improved and robustness level was recovered close to initial values.

3.3. Local dose differences

Fig. 5 presents near maximum dose errors (DEvol = 2%) in four different regions: prescription (> 95%Dp), high (65–95%Dp), medium (35–65%Dp) and low (< 35%Dp) dose levels. Dose restoration could reproduce the dose with high accuracy and precision in the whole pa-tient volume, with Median(DEvol = 2%) < 4 Gy in all dose level volumes. Dose differences between not adapted and restored doses were statistically significant (p < 0.05) in all regions for both rCTs.

Median(DEvol = 2%) of the entire dose region was decreased from 9.2[5.2] Gy (rCT1) and 8.2[4.7] Gy (rCT2) in the not adapted plans to 3.1[2.3] Gy (rCT1) and 2.9[1.7] Gy (rCT2) in the restored plans. Additionally, dose restoration precision, represented by the IQR, was decreased by a factor two respect to not adapted plans.

4. Discussion

In this study, the clinical value of the DR tool for lung IMPT ac-counting for inter-fractional density changes, in order to reduce the need of offline adaptation was evaluated. We observed that introducing DR reduced offline adaptation rate from 36%(5/14) to 7%(1/14).

Fast and accurate DR will be sufficient for the majority of the clinical cases. However, issues such as (1) changes in the relative

positions of anatomic structures or (2) poor quality registrations may cause an imperfect overlap between rigidly mapped and real contours. In such cases, the positive effects of DR will be less noticeable despite a successful reproduction of the initial dose, since it will be reconstructed in the wrong location. The first issue is not unique to PT, it could be solved as in XT, using a more comprehensive offline adaptation in-cluding re-contouring. For online adaptation, extensive quality assur-ance (QA) of tools as auto-contouring [32,33] or automated planning techniques [34,35] would be needed. A possible solution for (2) could be other registration strategies such as soft-tissue or carina-based po-sitioning [36]. Bony registration could be preferred in current practice for ensuring correct alignment of the bones with respect to proton paths and avoid dose distortions. However, soft tissue or carina based posi-tioning could be implemented safely due to inherent corrections brought by restoration.

Based on local dose differences analysis, regions of prescribed dose consistently showed better performance with the lowest Median (DEvol = 2%) = 1.7 Gy in restored plans. These results, together with the Median(DE(2%vol) < 4 Gy for entire dose region, were consistent with Median(DE(2%vol)) < 5 Gy obtained by Bernatowicz et al. [25].

Uncertainty sources such as motion, setup and range errors were included in the dose restoration robust re-optimization. Dose restora-tion could improve nominal and worst-case DVH-metrics in RS_map as well as in RS_real respect to no adaptation. Lower differences in worst-case values from the DVH-bands of restored plans indicated that adapted plans were more robust than not adapted plans.

Interplay effect was not addressed in this study since it is not a problem specific to dose restoration but to IMPT for mobile-targets in general. Issues associated to interplay have been studied and well known solutions such as re-scanning have been proposed in the litera-ture to compensate this effect [28,37,38,39].

As investigated in Van Der Voort et al. [16] for oropharyngeal cancer, the magnitude of range and setup robustness parameters can be approximated as a function of systematic and random uncertainties.
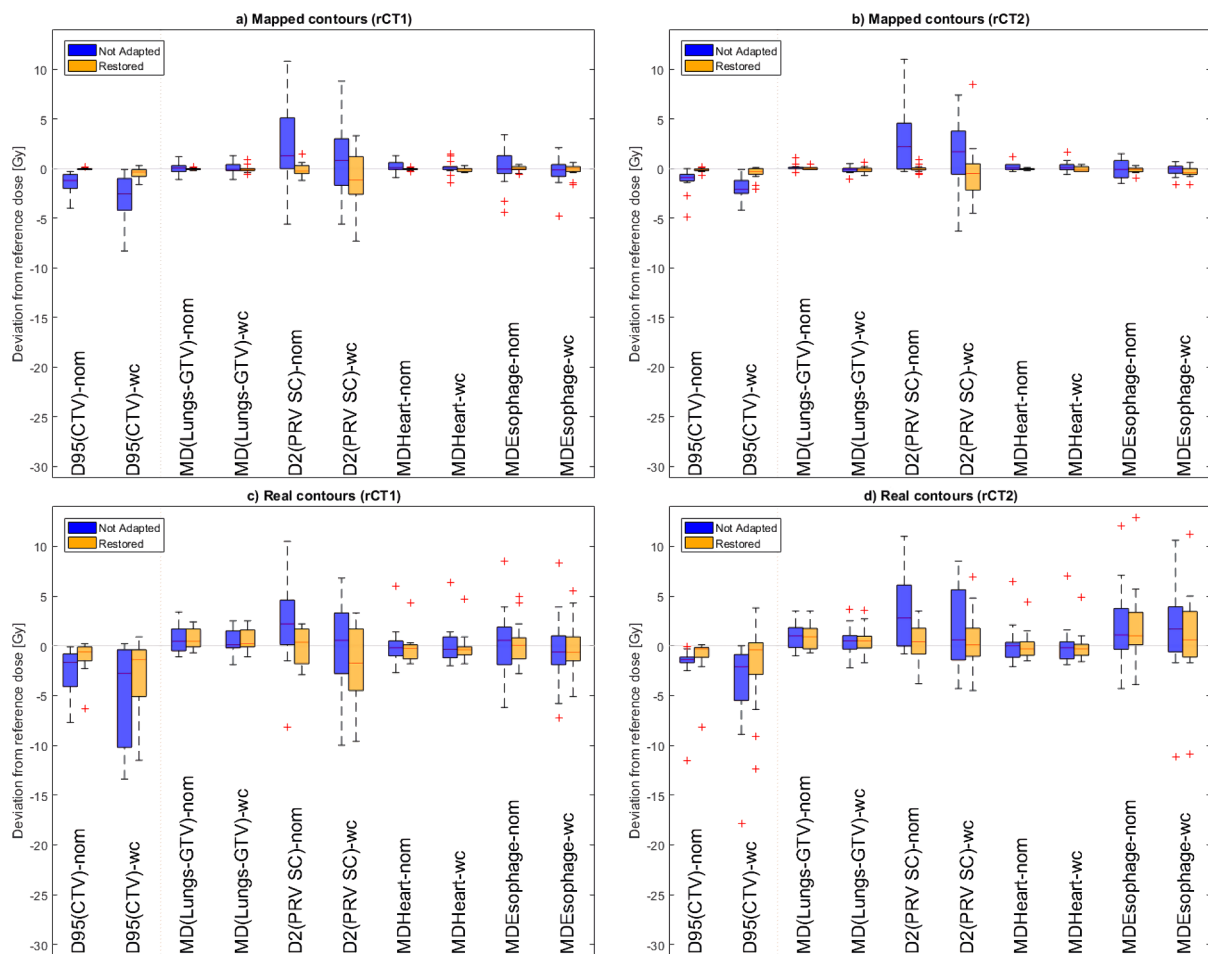
Fig. 3. Differences respect to the reference dose in nominal and worst-case metrics reported from DVH-bands were represented using boxplots. The median calculated among fourteen patients is shown by the horizontal line within boxes. Results were evaluated for both repeated-CTs(rCT1,rCT2) in two contours sets : mapped contours (RS_map) a),b) and real contours (RS_real) c),d). Abbreviations: *nom = nominal, wc = worst case, MD = mean dose, D2 = D2% dose received at 2% of the volume; PRV SC = Spinal Cord.*

Table 1

Summary of Wilcoxon's signed rank test p-values in the two contours sets : mapped contours (RS_maps) and real contours (RS_real) for both repeated-CTs (rCT1, rCT2). *Abbreviations : nom = nominal, wc = worst case, D95(CTV) = dose received at 95% of the CTV, MD = mean dose, D2(SpinalCord) = dose received at 2% of the volume of the spinal cord.*

	Mapped contours (RS_map)		Real contours (RS_real)	
	p (rCT1)	p (rCT2)	p (rCT1)	p (rCT2)
D95(CTV)-nom	0.0001	0.0010	0.0002	0.0005
D95(CTV)-wc	0.0005	0.0024	0.0295	0.0029
MD(Lung-GTV)-nom	0.6533	0.9063	0.8325	0.6914
MD(Lung-GTV)-wc	0.9679	0.6328	0.9883	0.8926
D2(SpinalCord)-nom	0.0166	0.0134	0.0580	0.0269
D2(SpinalCord)-wc	0.1465	0.2163	0.0906	0.2930
MD(Heart)-nom	0.1328	0.0811	0.2251	0.3955
MD(Heart)-wc	0.1851	0.1230	0.2578	0.2490
MD(Esophagus)-nom	0.9863	0.6563	0.7494	0.7764
MD(Esophagus)-wc	0.9604	0.3696	0.8394	0.5049

Hence, by increasing the initial plan robustness, less adaptation should be required. The implementation of an online adaptive workflow with dose restoration opens the possibility to reduce margins and/or decrease robustness parameters, compared to non-adaptive workflows. However, the relationship between the robustness parameters and the adaptation rate must be studied carefully on a suitable patient cohort.

Using dose restoration, the initial plan was adapted to the new patient density. The original plan was preserved (beam arrangement, target volumes) whilst re-optimization allows for modifications in proton energies and spot weights in order to reproduce the original dose. Keeping the reference dose distribution unchanged is the key to minimize the physician's approval step in a fully online adaptive workflow. However, despite restoring the approved planned dose, online adaptation requires modification of the pretreatment patient-specific QA procedure. For instance, a previous QA could be performed using a fast-independent dose calculation, followed by a more extensive analysis using machine log files after delivery [40,41,42]. Both procedures (pre/post treatment) could identify patients that require offline adaptation because of anatomical changes that DR cannot account for.

Clinical implementation of DR, will mostly impact the workload at the planning stage since the IBO plan needs to be optimized. Pencil Beam dose engine was used to speed up the workflow since Monte Carlo optimization was not needed to prove the suitability of the method, which focused more on the clinical feasibility of automating the process than on speed. DR workflow was able to generate plans of acceptable quality (accounting for density changes), in around 30 min [28 min 20 s – 31 min 21 s]. Since re-optimization is the most time demanding step, advanced optimization techniques, as scenario selection [43] and added computational power can make the time scale compatible with typical online treatment settings.

By routinely acquiring high quality patient volumetric images (e.g. in-room CT on rails), systematic setup errors can be mostly mitigated,
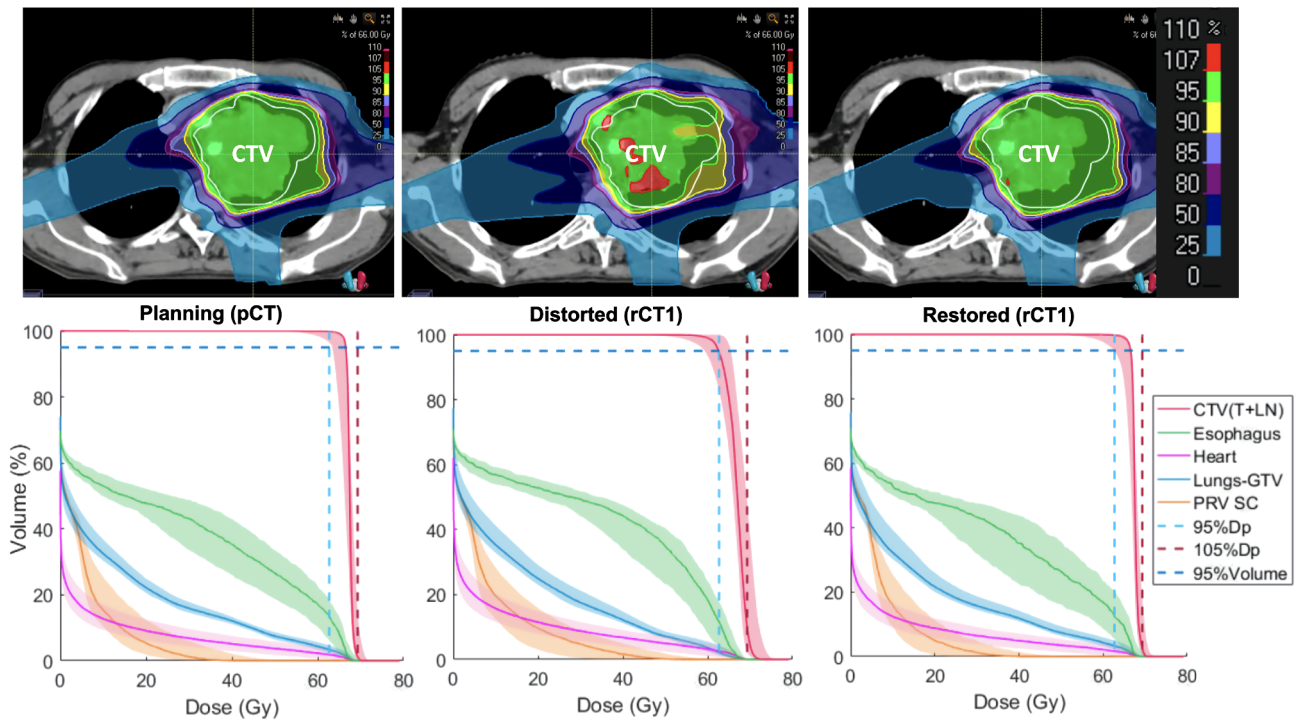
Fig. 4. Patient 9. DVH-bands resulting from the robustness tests are presented together with their corresponding nominal dose distributions. The continuous line represents the nominal scenario while the band collects the information from the evaluated uncertainty scenarios. The dashed lines represent the clinical limits (D95% > 95%Dprescribed). The pair of results (dose distribution/DVH-bands) are shown for the initial IBO plan (in the planning CT), the not adapted and the restored plans (in the first repeated-CT). *Abbreviations: pCT = planning-CT, rCT1 = first repeated-CT, rCT2 = second repeated-CT; CTV(T + LN) = CTV(tumor and nodes); PRV SC = Spinal Cord; Dp = Prescribed dose. (PRINTED IN COLOUR).*
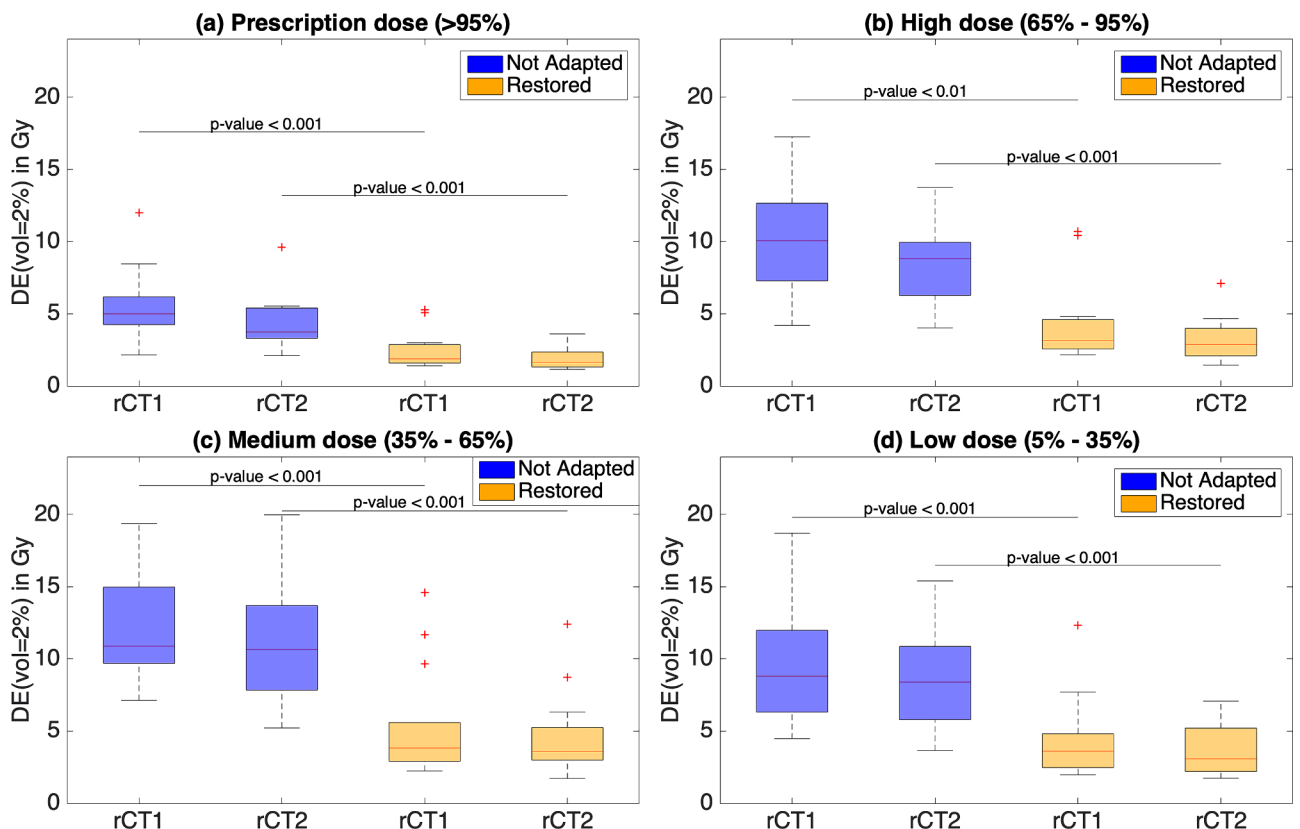

Fig. 5. Absolute dose error respect to the reference dose in small volumes DE(vol = 2%) represented in boxplots for 4 different regions corresponding to prescription, high, medium and low dose levels. Abbreviations: rCT1 = first repeated-CT, rCT2 = second repeated-CT.

allowing DR to deal primarily with the range errors. However, on-board CBCT could also be considered, but this requires advanced image quantification features in order to use CBCT information for dose computation [44,45,46].

Dose differences between not adapted and restored plans were statistically significant (p < 0.05) in all dose regions, the target volume and the spinal cord. No statistical signification was found for heart, lung and esophagus. However, this is not surprising since dose deviations between not adapted and planned dose distributions were in general small in organs-at-risk. In addition, it must be noted that patients who did not need adaptation were also included in our statistical analysis. More statistically significant results could have been achieved if we had included only patients that needed adaptations. Yet, we achieve statistical significance for target volumes, all dose regions, and the spinal cord.

Finally, it is worth mentioning that performing fast and accurate DR improved CTV coverage for all patients in comparison with no adaptation. DR key objective was to meet the planning criteria set by the radiation oncologists which were judged as clinically relevant. Since restoration allowed to get closer to the validated initial plan, and sometimes reestablish the planning criteria, this improvement is, by definition, clinically relevant. Ideally, dose restoration could be considered as standard clinical practice, in the same way as daily registration based on volumetric images.

In conclusion, this study showed that most of the investigated lung cases would benefit from an accurate dose restoration. This online adaptive workflow (based on repeated-CTs) did not require new organ and target segmentation nor contour deformation. Dose restoration was validated in rigidly mapped contours as well as in the real contours delineated by the physician. DVH-metrics and robustness were improved by DR in the new patient anatomy compared to no adaptation.

Declaration of Competing Interest

The authors declare that they have no known competing financial interests or personal relationships that could have appeared to influence the work reported in this paper.

Acknowledgement

Appendix A. Supplementary data

Supplementary data to this article can be found online at https://doi.org/10.1016/j.phro.2020.06.004.

References

[1] Kesarwala AH, Ko CJ, Ning H, Xanthopoulos E, Haglund KE, O'Meara WP, et al. Intensity-modulated proton therapy for elective nodal irradiation and involvedfield radiation in the definitive treatment of locally advanced non–small-cell lung cancer: a dosimetric study. Clin Lung Cancer 2015;16:237–44. https://doi.org/10.1016/j.cllc.2014.12.001.

[2] Ferris MJ, Martin KS, Switchenko JM, Kayode OA, Wolf J, Dang Q, et al. Sparing Cardiac Substructures With Optimized Volumetric Modulated Arc Therapy and Intensity Modulated Proton Therapy in Thoracic Radiation for Locally Advanced Non-small Cell Lung Cancer. Pract Radiat Oncol 2019;9:e473–81. https://doi.org/10.1016/j.prro.2019.04.013.

[3] Nichols RC, Huh SN, Henderson RH, Mendenhall NP, Flampouri S, Li Z, et al. Proton radiation therapy offers reduced normal lung and bone marrow exposure for patients receiving dose-escalated radiation therapy for unresectable stage iii non-smallcell lung cancer: a dosimetric study. Clin Lung Cancer 2019;12:252–7. https://doi.org/10.1016/j.cllc.2011.03.027.

[4] Teoh S, Fiorini F, George B, Vallis KA, Van den Heuvel F. Proton vs photon: A model-based approach to patient selection for reduction of cardiac toxicity in locally advanced lung cancer. Radiother Oncol 2019;S0167–8140(19):32973–81. https://doi.org/10.1016/j.radonc.2019.06.032.

[5] Chang JY, Li H, Ronald Zhu X, Liao Z, Zhao L, Liu A, et al. Clinical implementation of intensity modulated proton therapy for thoracic malignancies. Int J Oncol*Biol*Phys 2014;90(4):809–18. https://doi.org/10.1016/j.ijrobp.2014.07.045.

[6] Chang JY, Zhang W, Komaki R, Choi NC, Chan S, Gomez D, et al. Long-term outcome of phase I/II prospective study of dose-escalated proton therapy for early-stage non-small cell lung cancer. Radiother Oncol 2017;122:274–80. https://doi.org/10.1016/j.radonc.2016.10.022.

[7] Ho JC, Li H, Allen PK, Zhang X, Liao Z, Zhu XR, Gomez DR, Lin SH, Gillin MT, Komaki RU, Hahn SM, Chang JY. Clinical Outcome of Intensity Modulated Proton Therapy for Non-Small Cell Lung Cancer. Int J Radiat Oncol *Biol*Phys 2015;93(3):S188. https://doi.org/10.1016/j.ijrobp.2015.07.450.

[8] Makita C, Nakamura T, Takada A, Takayama K, Suzuki M, Azami Y, et al. High-dose proton beam therapy for stage I non-small cell lung cancer: Clinical outcomes and prognostic factors. Acta Oncol 2015;54:307–14. https://doi.org/10.3109/0284186X.2014.948060.

[9] Elhammali A, Blanchard P, Yoder A, Liao Z, Zhang X, Zhu XR, et al. Clinical outcomes after intensity-modulated proton therapy with concurrent chemotherapy for inoperable non-small cell lung cancer. Radiother Oncol 2019;136:136–42. https://doi.org/10.1016/j.radonc.2019.03.029.

[10] Higgins KA, O'Connell K, Liu Y, Gillespie TW, Mc-Donald MW, Pillai RN, et al. National cancer database analysis of proton versus photon radiation therapy in non-small cell lung cancer. Int J Radiat Oncol *Biol*Phys 2017;97(1):128–37. https://doi.org/10.1016/j.ijrobp.2016.10.001.

[11] Lomax AJ. Intensity modulated proton therapy and its sensitivity to treatment uncertainties 1: the potential effects of calculational uncertainties. Phys Med Biol 2008;53(4):1027–42. https://doi.org/10.1088/0031-9155/53/4/014.

[12] Lomax AJ. Intensity modulated proton therapy and its sensitivity to treatment uncertainties 2: the potential effects of inter-fraction and inter-field motions. Phys Med Biol 2008;53(4):1043–56. https://doi.org/10.1088/0031-9155/53/4/015.

[13] Liu W, Zhang X, Li Y, Mohan R. Robust optimization of intensity modulated proton therapy. Med Phys 2012;39(2):1079–91. https://doi.org/10.1118/1.3679340.

[14] Pflugfelder D, Wilkens JJ, Oelfke U. Worst case optimization: a method to account for uncertainties in the optimization of intensity modulated proton therapy. Phys Med Biol 2008;53:1689–700. https://doi.org/10.1088/0031-9155/53/6/013.

[15] Fredriksson A, Forsgren A, Hardemark B. Minimax optimization for handling range and setup uncertainties in proton therapy. Med Phys 2011;2011(38):1672–84. https://doi.org/10.1118/1.3556559.

[16] van der Voort S, van de Water S, Perkó Z, Heijmen B, Lathouwers D, Hoogeman M. Robustness Recipes for Minimax Robust Optimization in Intensity Modulated Proton Therapy for Oropharyngeal Cancer Patients. Int J Radiat Oncol *Biol*Phys 2016;95(1):163–70. https://doi.org/10.1016/j.ijrobp.2016.02.035.

[17] Li H, Zhang X, Park P, Liu W, Chang J, Liao Z, et al. Robust optimization in intensity-modulated proton therapy to account for anatomy changes in lung cancer patients. Radiother Oncol 2015;114(3):367–72. https://doi.org/10.1016/j.radonc.2015.01.017.

[18] Grassberger C, Dowdell S, Lomax A, Sharp G, Shackleford J, Choi N, et al. Motion interplay as a function of patient parameters and spot size in spot scanning proton therapy for lung cancer. Int J Radiat Oncol *Biol*Phys 2013;86(2):380–6. https://doi.org/10.1016/j.ijrobp.2013.01.024.

[19] Kardar L, Li Y, Li X, Li H, Cao W, Chang JY, et al. Evaluation and mitigation of the interplay effects of intensity modulated proton therapy for lung cancer in a clinical setting. Pract Radiat Oncol 2014;4(6):e259–68. https://doi.org/10.1016/j.prro.2014.06.010.

[20] Szeto YZ, Witte MG, Van Kranen SR, Sonke JJ, Belderbos J, Van Herk M. Effects of anatomical changes on pencil beam scanning proton plans in locally advanced nsclc patients. Radiother Oncol 2016;120(2):286–92. https://doi.org/10.1016/j.radonc.2016.04.002.

[21] Hoffmann L, Alber M, Jensen MF, Holt MI, Moller DS. Adaptation is mandatory for intensity modulated proton therapy of advanced lung cancer to ensure target coverage. Radiother Oncol 2017;122(3):400–5. https://doi.org/10.1016/j.radonc.2016.12.018.

[22] Green OL, Henke LE, Hugo GD. Practical Clinical Workflows for Online and Offline Adaptive Radiation Therapy. Sem Radiat Oncol 2019;29(3):219–27. https://doi.org/10.1016/j.semradonc.2019.02.004.

[23] Moore KL. Automated Radiotherapy Treatment Planning. Sem Radiat Oncol 2019;29(3):209–18. https://doi.org/10.1016/j.semradonc.2019.02.003.

[24] Jagt T, Breedveld S, Van de Water S, Heijmen B and Hoogeman M. Near real-time automated dose restoration in IMPT to compensate for daily tissue density variations in prostate cancer. Phys Med Biol 2017; 62(11):4254-4272. https://doi.org/10.1088/1361-6560/aa5c12.

[25] Bernatowicz K, Geets X, Barragan A, Janssens J, Souris K, Sterpin E. Feasibility of online IMPT adaptation using fast, automatic and robust dose restoration. Phys Med Biol 2018;63(8):085018 https://doi.org/10.1088/1361-6560/aaba8c.

[26] De Ruysscher D, Faivre-Finn C, Moeller D, Nestle U, Hurkmans CW, Le Pechoux C, et al. European organization for research and treatment of cancer (eortc) recommendations for planning and delivery of high-dose, high precision radiotherapy for lung cancer. Radiother Oncol 2017;124(1):1–10. https://doi.org/10.1016/j.radonc.2017.06.003.

[27] Inoue T, Widder J, van Dijk LV, Takegawa H, Koizumi M, Takashina M, et al. Limited impact of setup and range uncertainties, breathing motion, and interplay effects in robustly optimized intensity modulated proton therapy for stage iii non-small cell lung cancer. Int J Radiat Oncol*Biol*Phys 2016;96(3):661–9. https://doi.org/10.1016/j.ijrobp.2016.02.2454.

[28] Liu W, Schild SE, Chang JY, Liao Z, Chang Y-H, Wen Z, Shen J, Stoker JB, Ding X, Hu Y, Sahoo N, Herman MG, Vargas C, Keole S, Wong W, Bues M. Exploratory Study of 4D versus 3D Robust Optimization in Intensity Modulated Proton Therapy for

Lung Cancer. Int J Radiat Oncol*Biol*Phys 2016;95(1):523–33. https://doi.org/10.1016/j.ijrobp.2015.11.002.

[29] Wanet M, Sterpin E, Janssens G, Delor A, Lee JA, and Geets X. Validation of the mid-position strategy for lung tumors in helical tomotherapy. Radiotherapy and Oncology 2013(106), pp. S314–S315, 2013. 2nd ESTRO Forum 19–23 Geneva Switzerland April 2013 Doi: 10.1016/j.radonc.2013.10.025.

[30] Zhang M, Zou W, Kevin Teo BK. Image guidance in proton therapy for lung cancer. Transl Lung Cancer Res 2018;7(2):160–70. https://doi.org/10.21037/tlcr.2018.03.26.

[31] Landry G, Hua C. Current state and future applications of radiological image guidance for particle therapy. Med Phys 2018;45(11):e1086–95. https://doi.org/10.1002/mp.12744.

[32] Van der Veen J, Willems S, Deschuymer S, Robben D, Crijns W, Maes F, et al. Benefits of deep learning for delineation of organs at risk in head and neck cancer. Radiother Oncol 2019;138:68–74. https://doi.org/10.1016/j.radonc.2019.05.010.

[33] Yun J, Yip E, Gabos Z, Wachowicz K, Rathee S, Fallone BG. Neural-network based autocontouring algorithm for intrafractional lung-tumor tracking using Linac-MR. Med. Phys 2015;42:2296–310. https://doi.org/10.1118/1.4916657.

[34] Nguyen D, Jia X, Sher D, Lin MH, Iqbal Z, Liu H, et al. 3D radiotherapy dose prediction on head and neck cancer patients with a hierarchically densely connected U-net deep learning architecture. Phys Med Biol 2019;64:065020 https://doi.org/10.1088/1361-6560/ab039b.

[35] Barragan-Montero AM, Nguyen D, Lu W, Lin MH, Norouzi-Kandalan R, Geets X, et al. Three-dimensional dose prediction for lung IMRT patients with deep neural networks: robust learning from heterogeneous beam configurations. Med Phys 2019;46:3679–91. https://doi.org/10.1002/mp.13597.

[36] Molitoris KJ, Diwanji T, Snider 3rd JW, Mossahebi S, Samanta S, Badiyan SN, et al. Advances in the use of motion management and image guidance in radiation therapy treatment for lung cancer. J Thoracic Dis 2018;10(Suppl 21):S2437–50. https://doi.org/10.21037/jtd.2018.01.155.

[37] Knopf AC, Hong TS, Lomax A. Scanned protonradiotherapy for mobile targets - the effectiveness of re-scanning in the context ofdifferent treatment planning approaches and for different motion characteristics. Phys Med Biol 2011;56(22):7257–71. https://doi.org/10.1088/0031-9155/56/22/016.

[38] Zhang Y, Huth I, Wegner M, Weber DC, Lomax A. An evaluation of rescanning technique for liver tumour treatments using a commercial pbs proton therapy system. Radiother Oncol 2016;121(2):281–7. https://doi.org/10.1016/j.radonc.2016.09.011.

[39] Kardar L, Li Y, Li X, Li H, Cao W, Chang JY, et al. Evaluation and mitigation of the interplay effects of intensity modulated proton therapy for lung cancerin a clinical setting. Pract Radiat Oncol 2014;4(6):259–68. https://doi.org/10.1016/j.prro.2014.06.010.

[40] Li H, Sahoo N, Poenisch F, Suzuki K, Li Y, Li X, et al. Use of treatment log files in spot scanning proton therapy as part of patient-specific quality assurance. Med Phys 2013;40:021703 https://doi.org/10.1118/1.4773312.

[41] Meier G, Besson R, Nanz A, Safai S, Lomax AJ. Independent dose calculations for commissioning, quality assurance and dose reconstruction of PBS protontherapy. Phys Med Biol 2015;60(7):2819–36. https://doi.org/10.1088/0031-9155/60/7/2819.

[42] Zhu XR, Li Y, Mackin D, Li H, Poenisch F, Lee AK, et al. Towards Effective and Efficient Patient-Specific Quality Assurance for Spot Scanning Proton Therapy. Cancers 2015;7(2):631–47. https://doi.org/10.3390/cancers7020631.

[43] Buti G, Souris K, Barragan Montero AM, Lee JA, Sterpin E. Towards fast and robust 4d optimization for moving tumors with scanned proton therapy. Med Phys 2019;46(12):5434–43. https://doi.org/10.1002/mp.13850.

[44] Kurz C, Nijhuis R, Reiner M, Ganswindt U, Thieke C, Belka C, et al. Feasibility of automated proton therapy plan adaptation for head and neck tumors using cone beam CT images. Radiat Oncol 2016;11:64. https://doi.org/10.1186/s13014-016-0641-7.

[45] Veiga C, Janssens G, Teng C-L, Baudier T, Hotoiu L, McClelland JR, Royle G, Lin L, Yin L, Metz J, Solberg TD, Tochner Z, Simone II CB, McDonough J, Kevin Teo B-K. First Clinical Investigation of Cone Beam Computed Tomography and Deformable Registration for Adaptive Proton Therapy for Lung Cancer. Int J Radiat Oncol*Biol*Phys 2016;95(1):549–59. https://doi.org/10.1016/j.ijrobp.2016.01.055.

[46] Thummerer A, Zaffino P, Meijers A, Guterres Marmitt G, Seco J, Steenbakkers RJHM, et al. Comparison of CBCT based synthetic CT methods suitable for proton dose calculations in adaptive proton therapy. Phys Med Biol 2020;65(9):095002 https://doi.org/10.1088/1361-6560/ab7d54.